JOURNAL OF SOLID STATE CHEMISTRY 73, 160–171 (1988)

Relation Structure–Fast Ion Conduction in the NASICON Solid Solution

J. P. BOILOT

Groupe de Chimie du Solide, Laboratoire de Physique de la Matière Condensée, Ecole Polytechnique, Palaiseau Cedex 91128, France

G. COLLIN

Laboratoire de Physique des Solides, Université Paris-Sud Bt. 510, Orsay 91405, France

AND PH. COLOMBAN

Groupe de Chimie du Solide, Laboratoire de Physique de la Matière Condensée, Ecole Polytechnique, Palaiseau Cedex 921128, France

Received April 15, 1987; in revised form July 6, 1987

Crystal determinations of the rhombohedral phase (space group $R\bar{3}c$), for different compositions ($2 < x < 2.4$) in the true NASICON solid solution $Na_{1+x}Zr_2Si_xP_{3-x}O_{12}$, have been performed at different temperatures by X-ray diffraction. We observe, as a consequence of interionic repulsions, the partial occupation of a mid-Na interstitial site within the conduction path. The composition dependence of the mid-Na occupation factor, maximum at $x = 2$, explains the maximum of the c hexagonal parameter and of the Na(1)–oxygen average distance observed at about $x = 2$. Moreover, structural results clearly suggest that the enhanced conductivity at $x = 2$ arises from sodium interactions instead of geometry changes of the framework. © 1988 Academic Press, Inc.

Introduction

Fast ion conduction in solid solutions between sodium zirconium phosphate and sodium zirconium silicate, $Na_{1+x}Zr_2Si_xP_{3-x}O_{12}$ ($0 \leq x \leq 3$), was first reported by Hong (*1*) and by Goodenough *et al.* (*2*). The two end member compositions (i.e., $x = 0$ and $x = 3$) have high resistivities. In contrast, polycrystalline samples with compositions $1.8 < x < 2.4$ exhibit a low resistivity which is minimum for $x = 2$ (about 3 Ω cm at 300°C) (*2–6*) (Fig. 1). For instance, the transport properties of $Na_3Zr_2Si_2PO_{12}$ ($x = 2$), a composition called NASICON (sodium super ionic conductor), are clearly equivalent to those of β'' alumina.

The general features of the NASICON-type packing, in the rhombohedral symmetry ($R\bar{3}c$), have been known for many years from crystal structure determinations of both end members $x = 0$ (*1*, *7*) and $x = 3$ (*8*, *9*). The robust three-dimensional framework is formed by fundamental groups consisting of two ZrO_6 octahedra and three SiO_4/PO_4 tetrahedra with which they share

0022-4596/88 $3.00

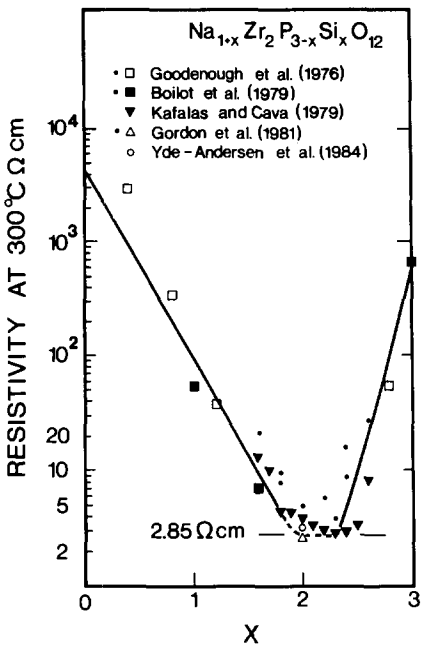

FIG. 1. Resistivity versus composition at 300°C for Na^+ in NASICON ceramics (adapt from Ref. (*6*)).

corner oxygen. Sodium ions occupy three-dimensional interstices: all the octahedral interstices noted Na(1) in pure phosphate ($x = 0$) and also all the irregular 8-coordinated Na(2) in pure silicate ($x = 3$). There is respectively one Na(1) and three Na(2) by unit formula $Na_{1+x}Zr_2Si_xP_{3-x}O_{12}$.

In fact, since its initial discovery, there has been extensive discussion about the "true" stoichiometry of NASICON. Different formulae were proposed such as

$$Na_{1+4y+x}Zr_{2-y}Si_xP_{3-x}O_{12} \text{ (}10, 11\text{)}$$

and

$$Na_{1+4y+x}Zr_{2-y-z}Si_xP_{3-x}O_{12-2z} \text{ (}12\text{)}.$$

This reflects difficulties during the preparation of the powders and of the crystals such as free zirconia precipitation, P_2O_5 and Na_2O losses, glassy phase formation, incongruent melting . . . , which suggests that the observed stoichiometric differences can be attributed to the different paths by which each NASICON was prepared: high-temperature solid state reaction, hydrothermal, or sol–gel procedure (*13*). However, we have recently clearly demonstrated, from a crystal structure determination (*14*), the formation of $Na_{3.09(8)}Zr_{2.00(1)}P_{0.91}Si_{2.09}O_{12}$, which confirms the existence of the $Na_{1+x}Zr_2P_{3-x}Si_xO_{12}$ Hong solid solutions which only exhibit the Si–P nonstoichiometry mechanism.

In his fundamental paper, Hong (*1*) has shown that the variations in conductivity with composition were closely coupled with structural changes:

(a) First, all the compositions showing fast ionic sodium transport are characterized at room temperature by a slight monoclinic distortion (*B2/b*) of the ideal rhombohedral packing. In fact, it was later observed (*3, 15*) that the monoclinic low-temperature structure transforms into high-temperature rhombohedral structure, at temperature close to 400 K, via a structural phase transition.

(b) Second, upon substitution of the larger Si ion for P and associated insertion of charge-compensating sodium ions, the hexagonal a axis increases monotonically. In contrast, as x increases, the hexagonal (or pseudohexagonal) c parameter rises to a maximum near $x = 2$ and then therefore anomalously decreases up to $x = 3$.

(c) Finally, the high conductivity of NASICON was geometrically rationalized in terms of the dimensions of the window between Na(1) and Na(2) positions. The geometrical bottleneck for the diffusion is the triangle formed by the oxygens of the NaO_6 octahedron and the opening of the bottleneck seems to be associated with the increase of the c_{hex} parameter, maximum at $x \sim 2$.

The structural changes with variations in composition were then examined by Wuensh *et al.* (*16*) using Rietveld analysis of neutron powder diffraction data at room temperature. These authors investigated

the structure of two rhombohedral ($x = 1$ and $x = 2.5$) and of two monoclinic ($x = 1.6$ and $x = 2$) compounds. They found that the Na(1) site remains fully occupied and the excess x of sodium progressively fills the Na(2) sites. The principal changes in the framework with change in composition are distortion and increased rotation of the Si–P tetrahedra up to $x = 2$, followed by progressive return toward the original orientation for larger x. This rotation acts to increase the height of the Na(1) octahedra and is responsible for the anomalous maximum in the length of the c axis. The rotation also causes the windows along likely diffusion paths to increase to a maximum size, close to the ionic radius of Na^+, near $x = 2$.

Kohler *et al.* (*11, 17*) examined the diffusion path in the high-temperature phase for a Zr defective single crystal, $Na_{3.1}Zr_{1.78}P_{1.76}Si_{1.24}O_{12}$, using the results of joint probability density function (p.d.f.) They established that the most probable path, from Na(1) to Na(2), does not follow a straight line but has a zigzag shape. They observed that the opening of bottleneck increases when the temperature is raised, which is associated with the decrease of the potential barrier and the increase of the hexagonal c parameter. But p.d.f. revealed that the bottleneck does not correspond to the maximum barrier 0.19 eV at 614 K which is localized further in the conducting channel.

Finally, from our recent crystal structure determination of the true NASICON (*14*), we have detected a new sodium position (mid-Na) in the conduction channel, intermediate between the usual Na(1) and Na(2) sites. In fact, only at high temperature (500 K), a very weak occupation of this site has been previously observed by neutron diffraction (*18*) in the $Na_3Cr_2(PO_4)_3$ NASICON analog and also by NMR (*19*) in $NaZr_2(PO_4)_3$.

There are six mid-Na per unit formula in a five-fold coordinated polyhedron. Conduction channels ideally corresponding to infinite zigzag lines of identical segments (7 Å) with 3Π/4 bents are schematically represented in Fig. 2.

We present here X-ray single crystal determination of the rhombohedral phase for different compositions in the true NASICON solid solution (between $x = 2$ and $x = 2.4$). Emphasis is laid on the temperature and on the composition dependences of:

(i) the filling ratio of each sodium site (as there are at most 4 Na ions per unit formula

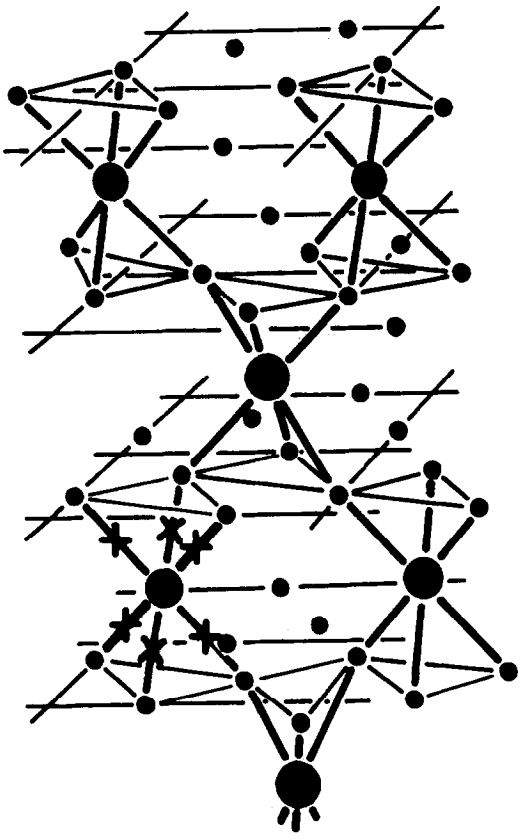

FIG. 2. Schematic representation of a part of the conduction channels in NASICON. The planes are on $z = \frac{1}{12}, \frac{3}{12}, \frac{5}{12}, \ldots$ in the hexagonal cell. Large circles correspond to Na(1) positions, small circles to Na(2) positions, and crosses to mid-Na positions (only six are indicated). A given Na(1) is connected to six mid-Na and six Na(2) positions. A given Na(2) is connected to two Na(1) positions.

within the conducting channels, it is clear that all positions cannot be occupied simultaneously);

(ii) the sodium–oxygen average distances;

(iii) the a and c hexagonal parameters.

These results show that the maximum of conductivity at $x = 2$ can be rationalized in terms of the sodium–sodium interactions. The framework of the structure mainly serves to define conducting channels.

Experimental

Single crystals of pure phosphate were obtained directly from the melt or by flux technique in boron oxide (*20*). Single crystals of various compositions ($2 < x < 2.4$) were prepared by graingrowth in sol–gel ceramics. As previously reported (*13*), a well-crystallized NASICON phase can be prepared by sol–gel technique after a thermal treatment above 1150°C. In fact, at this temperature, especially for compositions outside the $1.9 < x < 2.1$ range, ceramics consist of NASICON grains (a few micrometers in size) accompanied by a second phase (monoclinic zirconia or glass). Nevertheless, as shown in Fig. 3, by long thermal annealing just below the melting point (for instance 4 months at 1245°C), an abnormal growth of NASICON crystals is observed (dimensions of crystals are typically 100–300 μm). This has been related (*21*) to the high chemical purity of sol–gel ceramics which prevents the impurity concentration at the grain boundaries and consequently enhances the grain growth.

Crystal structure determinations have

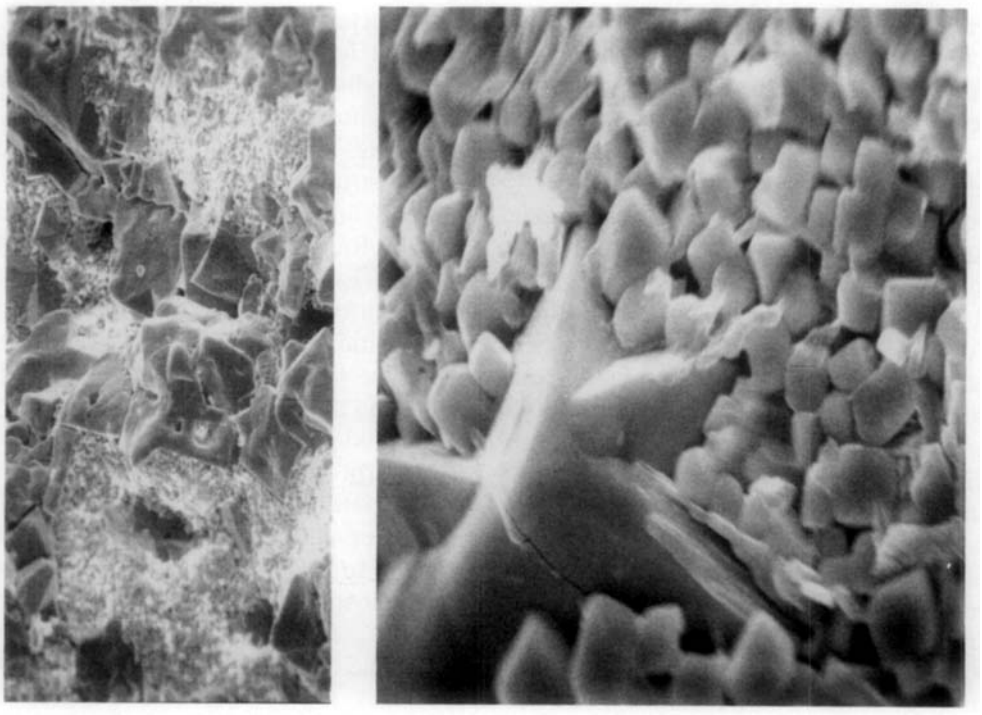

FIG. 3. Microstructure of NASICON sol–gel ceramics (at two scales) after long thermal treatment just below the melting temperature. Small crystals (100–300 μm) have grown beside small crystallites formed of NASICON and a second phase.

been performed at different temperatures by X-ray diffraction on several crystals of different compositions. In fact, we present here only the results concerning crystals in the rhombohedral phase, i.e., above the phase transition for compositions (around $x = 2$) exhibiting the monoclinic distortion. Details of crystal structure determination for the end member $x = 0$ at room temperature (in the rhombohedral phase) and descriptions of low-temperature monoclinic phase will be published elsewhere.

NASICON crystals are systematically twinned with respect to the rhombohedral average lattice: reflections such as $(-h + k + l) = 3n$ and $(h - k + k = 3n)$ in hexagonal notation are simultaneously present (observe and reverse description, respectively). For each crystal structure determination, data were collected using Mo$K\alpha$ radiation up to $2\theta = 65°$. After absorption corrections and averaging equivalent reflections, this led to about 700 independent reflections which all were used in the refinement, including the reflections with zero intensity. These reflections were corrected for anomalous dispersion (*22*) and the refinement program was modified in order to calculate structure factors in this special case of twinned crystals (*23*). Under these conditions, the refinements where carried out within the usual $R\bar{3}c$ space group of NASICON with simultaneous refinement of spatial coordinates, anisotropic temperature factors, and occupancies for the two usual Na(1) and Na(2) sodium sites. Refinements also included anharmonic corrections to the Debye–Waller factors up to the 4th order with full contravariant tensors for Na(1) and Na(2) and contracted contravariant pseudotensors for oxygen and zirconium atoms (*24*). As previously observed (*14*) for the first crystal structure determination of the true NASICON, further calculations reveal, for crystals in the composition range $2 < x < 2.4$, the occupation of a third sodium position within the conduction path, approximately halfway between ideal Na(1) and Na(2) positions (~1.8 Å from each one). The introduction of this position, previously labeled mid-Na (*14*), is always associated to a significant decrease (according to Hamilton statistical tests (*25*)) of the agreement factor defined as $R(\%) = 100^*\Sigma|F_{obs} - F_{calc}|/\Sigma F_{obs}$. For instance, the R factor decreases from 3.6 to 2.9% for the $x = 2.05$ NASICON at 623 K.

Results

Table I shows the investigated compositions, the recording temperature (for $x = 2.05$, 2.15, and 2.25, structural determinations have been performed at high temperature—443 and 623 K—because of the monoclinic distortion at room temperature; for $x = 0$ and $x = 2.35$, the rhombohedral phase exists at room temperature), the hexagonal parameters, the agreement factor, and the composition deduced from the refinement for each investigated sample. In order to discuss the structural changes with the variation of composition, the results obtained by Tran Qui *et al.* (*9*) from X-ray crystal structure determination for the $x = 3$ end member and by Baur *et al.* (*26*) from neutron Rietveld analysis for $x = 1$ are also given in Table I.

For all of the X-ray determinations, the compositions deduced from the refinement are close (although systematically slightly higher) to the values calculated by using the (P, Si) oxygen average distances and a linear interpolation between the two extreme values determined under the same experimental conditions: P–O = 1.524(1) Å and Si–O = 1.623(1) Å, respectively, from $x = 0$ pure phosphate end member and pure zircon silicate ($ZrSiO_4$).

For the compounds with compositions in the range $2 < x < 2.4$, the coordinates and thermal parameters obtained by X-ray crystal structure determinations are summarized in Table II.

TABLE I

CRYSTAL STRUCTURE DETERMINATION IN $Na_{1+x}Zr_2Si_xP_{3-x}O_{12}$: COMPOSITION ($x$), HEXAGONAL PARAMETERS (a, c), $Z = 6$, AND AGREEMENT FACTOR (R)

Sample reference	Recording temperature (°K)	a (Å)	c (Å)	x Value from the refinement	x Value from ⟨(Si,P)–O⟩	R (%) factor
$x = 0$	300	8.81	22.75			
$x = 0$[a]	443	8.80	22.83			
$x = 1$[b]	443	8.933(2)	22.925(3)			
$x = 2.05$	443	9.068(2)	22.980(4)	2.04(9)	2.00(9)	3.47
$x = 2.05$	623	9.074(2)	23.057(4)	2.09(8)	2.06(9)	2.93
$x = 2.15$	443	9.079(2)	22.964(4)	2.15(9)	2.06(9)	3.48
$x = 2.25$	443	9.084(2)	22.928(4)	2.27(9)	2.21(9)	2.96
$x = 2.25$	623	9.089(2)	23.000(4)	2.24(9)	2.18(9)	2.82
$x = 2.35$	300	9.097(2)	22.680(4)	2.37(12)	2.21(13)	5.76
$x = 3$[c]	443	9.200(1)	22.351(2)			

[a] Calculated by using linear thermal expansion coefficients (Ref. (*27*)) and values at 300 K.
[b] From Ref. (*26*), extrapolated from values at 293 and 573 K.
[c] From Ref. (*9*), extrapolated from values at 293 and 573 K.

(*i*) *Lattice Constants*

Refined lattice constant are compared in Table I in terms of hexagonal cells. Figure 4 shows the composition dependence at 443 K of the a and c parameters. As previously observed by Hong (*1*), the a hexagonal lattice constant monotonically increases with the progressive substitution of Si for P ions and insertion of Na^+. On the contrary, the length of the c parameter highly decreases between $x = 2$ and $x = 3$.

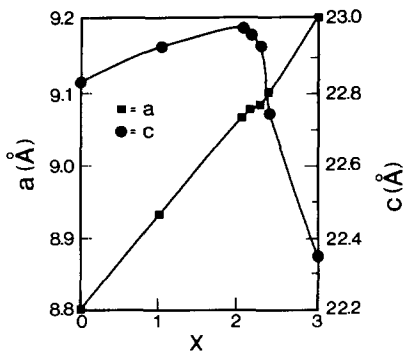

FIG. 4. Composition dependence at 443 K of the a and c hexagonal parameters in the NASICON solid solution $Na_{1+x}Zr_2Si_xP_{3-x}O_{12}$ with $0 \leq x \leq 3$ (crystal data except for $x = 1$; Ref. (*26*)).

The effective volume expansion coefficients determined in the temperature range 443–623 K are 2.7×10^{-5} °C^{-1} for $x = 2.05$ and 2.4×10^{-5} °C^{-1} for $x = 2.25$. Lattice constant determinations previously reported by Tran Qui *et al.* (*9*), for the silicate end member $x = 3.0$ provide a relatively close volume expansion coefficient of 3.7×10^{-5} °C^{-1}, in contrast with the phosphate end member which is well known to exhibit a low coefficient (-4×10^{-6} °C^{-1} (*3*, *27*). The corresponding linear thermal expansion coefficients—normal to c and parallel to c, respectively—are 4×10^{-6} and 1.9×10^{-5} °C^{-1} for $x = 2.25$, to be compared with $<10^{-7}$ and 3.7×10^{-5} °C^{-1} for the pure silicate (*9*) and with -6×10^{-6} and 2.5×10^{-5} °C^{-1} for pure phosphate (*27*). Therefore, as a function of the composition, small thermal changes are observed along the c axis and the variation of the volume expansion is essentially due to changes along the a axis.

TABLE II

COORDINATES (×10⁴) AND THERMAL PARAMETERS (Å² × 10⁴)

	Max. occup.[a]	occup.[b]	x	y	z	U_{eq}
			NASICON x = 2.05 at 443 K			
Zr	2	2.00(1)	0	0	1478(1)	151(2)
P–Si	3	3	2903(1)	0	¼	135(5)
O(1)	6	6	1724(4)	−344(5)	1946(1)	363(14)
O(2)	6	6	1932(3)	1696(3)	914(1)	273(11)
Na(1)	1	0.36(2)	0	0	0	1248(113)
Na(2)	3	2.01(2)	6347(7)	0	¼	986(77)
mid-Na	6	0.67(5)	9853(51)	8066(89)	9798(20)	2183(520)
			NASICON x = 2.05 at 623 K			
Na(1)	1	0.40(2)	0	0	0	2152(230)
Na(2)	3	2.05(2)	6345(5)	0	¼	1053(70)
mid-Na	6	0.64(4)	9764(46)	7958(60)	9773(35)	2000(400)
			NASICON x = 2.15 at 443 K			
Zr	2	2.00(1)	0	0	1479(1)	151(1)
P–Si	3	3	2906(1)	0	¼	142(6)
O(1)	6	6	1736(5)	−333(5)	1942(2)	368(16)
O(2)	6	6	1930(4)	1698(4)	911(1)	271(12)
Na(1)	1	0.32(1)	0	0	0	944(112)
Na(2)	3	2.15(3)	6342(7)	0	¼	1112(81)
mid-Na	6	0.68(5)	9778(58)	8082(64)	9787(24)	1976(404)
			NASICON x = 2.25 at 443 K			
Zr	2	2.00(1)	0	0	1478(1)	152(1)
P–Si	3	3	2909(1)	0	¼	137(4)
O(1)	6	6	1738(3)	−325(4)	1943(1)	353(12)
O(2)	6	6	1919(3)	1689(3)	910(1)	271(9)
Na(1)	1	0.36(2)	0	0	0	882(92)
Na(2)	3	2.24(3)	6352(4)	0	¼	1011(64)
mid-Na	6	0.67(4)	9782(44)	8111(65)	9800(18)	1820(360)
			NASICON x = 2.25 at 623 K			
Na(1)	1	0.37(2)	0	0	0	1683(146)
Na(2)	3	2.26(3)	6346(6)	0	¼	1171(68)
mid-Na	6	0.61(4)	9739(39)	7968(57)	9756(21)	1809(440)
			NASICON x = 2.35 at 300 K			
Zr	2	2.01(2)	0	0	1475(1)	114(4)
P–Si	3	3	2921(2)	0	¼	153(9)
O(1)	6	6	1777(7)	−281(7)	1936(3)	382(26)
O(2)	6	6	1902(5)	1672(5)	898(3)	243(20)
Na(1)	1	0.49(2)	0	0	0	488(66)
Na(2)	3	2.32(4)	6371(6)	0	¼	721(50)
mid-Na	6	0.56(6)	9655(52)	7810(120)	9756(32)	1800(350)

Note. U_{eq} is defined by the expression $U_{eq}(Å^2) = \Sigma_{ij} U_{ij} a_i^* a_j^*$.

[a] Max. occup. = 6 refers to the 36f positions of the $R\bar{3}c$ group, max. occup. = 3 refers to the 18e positions, max. occup. = 2 to the 12c positions, and max. occup. = 1 to the 6b positions.

[b] Occupation corresponding to one $Na_{1+x}Zr_2Si_xP_{3-x}O_{12}$ formula.

All of the linear expansion coefficients determined near $x = 2$ are also in agreement with data obtained by neutron Rietveld analysis at 300 and 593 K for $x = 1.6$ and $x = 2$ by Didisheim *et al.* (*28*).

(ii) Site Occupancies

For the six crystal determinations, evidence of the total occupancy of the Zr octahedron is found, unambiguously demonstrating that our crystals belong to solid solution $Na_{1+x}Zr_2Si_xP_{3-x}O_{12}$ in which only the Si–P nonstoichiometry mechanism is present.

Sodium ions are distributed within the conduction channel in the three positions referred to as Na(1), Na(2), and mid-Na. In contrast with previous neutron Rietveld analysis, we find that the Na(1) interstice does not remain fully occupied whatever the composition is. However, it is clear that, for all compositions and all temperatures which have been investigated, one sodium ion per unit formula occupies either Na(1) site or mid-Na site and that the other x sodium ions in excess (charge compensation ions) occupy Na(2) sites. Therefore the compositions of all our single crystals are close to the following ideal formula:

$$(\text{Na(1)} + \text{mid-Na})_1(\text{Na(2)})_x\square_{3-x}Zr_2(P_{3-x}Si_x)O_{12} \quad \text{with} \quad 0 \le x \le 3.$$

This relation takes into account that occupation of mid-Na sites automatically excludes occupation of the neighboring Na(1).

Figure 5 shows the composition dependence of the sodium site occupancies. As

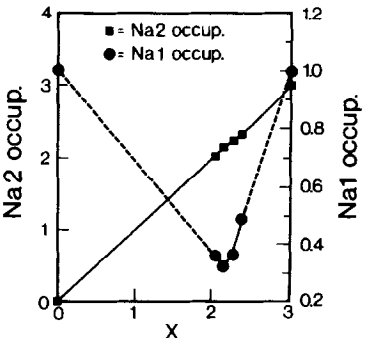

FIG. 5. Composition dependence at 443 K for the sodium site occupancies (Na(1) and Na(2)) deduced from the crystal study determinations in the NASICON solid solution $Na_{1+x}Zr_2Si_xP_{3-x}O_{12}$ with $0 \le x \le 3$.

TABLE III

AVERAGE INTERIONIC DISTANCES IN $Na_{1+x}Zr_2Si_xP_{3-x}O_{12}$

Sample ref.	Recording temp. (°K)	⟨Zr–6 × O⟩	⟨(Si,P)–4 × O⟩	⟨Na(1)–6 × O⟩	⟨Na(2)–8 × O⟩	⟨mid-Na–5 × O⟩
$x = 0$	300		1.524(1)	2.548(2)	2.648(4)	
$x = 1$[a]	443	2.071(2)	1.552(2)	2.639(2)	2.668(6)	
$x = 2.05$	443	2.076(2)	1.590(1)	2.672(2)	2.684(4)	2.46(2)
$x = 2.05$	623	2.076(2)	1.592(1)	2.688(2)	2.686(4)	2.48(2)
$x = 2.15$	443	2.077(2)	1.592(1)	2.669(2)	2.686(4)	2.47(2)
$x = 2.25$	443	2.072(2)	1.597(1)	2.659(2)	2.687(4)	2.48(2)
$x = 2.25$	623	2.076(2)	1.596(1)	2.675(2)	2.689(4)	2.48(1)
$x = 2.35$	300	2.071(2)	1.597(2)	2.612(4)	2.686(5)	2.46(3)
$x = 3$[b]	443	2.082(3)	1.623(3)	2.520(3)	2.706(4)	

[a] From Ref. (*26*), extrapolated from values at 293 and 573 K.
[b] From Ref. (*9*), extrapolated from values at 293 and 573 K.

expected from the previous dependence of the sodium site occupancies. As expected from the previous formula, we note a continuous increase of the Na(2) occupation when x increases. More interesting is that the Na(1) occupation and obviously the mid-Na occupation are clearly related to the variations in conductivity with composition. The Na(1) occupation decreases to a minimum (about $\frac{1}{3}$) near $x = 2$ and then anomalously increases up to 1 at $x = 3$.

Very weak temperature effects are observed. However, when the temperature increases, the Na(1) site occupancy slightly increases to the detriment of the mid-Na one and the mid-Na position slightly moves to the Na(2) position. For NASICON $x = 2.05$, the distance between two neighboring Na(2) and mid-Na sites varies from 1.88 Å at 443 K to 1.78 Å at 623 K. Obviously, these short distances forbid simultaneous occupation of these two positions.

(*iii*) *Interionic Distances*

Table III summarizes average interionic distances, deduced from the refinement, for different x values and Table IV shows significant interionic distances for NASICON $x = 2.05$ at 443 and 623 K.

As already observed in previous structural determinations, the Na(2)–oxygen distances are much longer than the value of 2.53 Å corresponding to the sum of the

TABLE IV

SIGNIFICANT INTERIONIC DISTANCES (Å) NASICON $x = 2.05$

At 443 K			
Zr–O(1)	3 × 2.048(2)	Na(1)–O(2)	6 × 2.672(2)
Zr–O(2)	3 × 2.103(2)	⟨Na(1)–O⟩	6 × 2.672
⟨Zr–O⟩	6 × 2.076		
		Na(2)–O(2)	2 × 2.476(3)
(Si–P)–O(1)	2 × 1.588(1)	Na(2)–O(2)	2 × 2.557(6)
(Si–P)–O(2)	2 × 1.591(1)	Na(2)–O(1)	2 × 2.807(3)
⟨(Si–P)–O⟩	4 × 1.590	Na(2)–O(1)	2 × 2.896(6)
		⟨Na(2)–O⟩	8 × 2.684
	mid-Na–O(2)	1 × 2.29(2)	
	mid-Na–O(1)	1 × 2.34(2)	
	mid-Na–O(2)	1 × 2.38(2)	
	mid-Na–O(2)	1 × 2.56(2)	
	mid-Na–O(1)	1 × 2.71(2)	
	mid-Na–O(2)	1 × 3.21(2)	
At 623 K			
Zr–O(1)	3 × 2.049(2)	Na(1)–O(2)	6 × 2.688(2)
Zr–O(2)	3 × 2.104(2)	⟨Na(1)–O⟩	6 × 2.688
⟨Zr–O⟩	6 × 2.076		
		Na(2)–O(2)	2 × 2.477(3)
(Si–P)–O(1)	2 × 1.592(1)	Na(2)–O(2)	2 × 2.561(6)
(Si–P)–O(2)	2 × 1.593(1)	Na(2)–O(1)	2 × 2.820(3)
⟨(Si–P)–O⟩	4 × 1.592	Na(2)–O(1)	2 × 2.888(6)
		⟨Na(2)–O⟩	8 × 2.686
	mid-Na–O(1)	1 × 2.33(2)	
	mid-Na–O(2)	1 × 2.33(2)	
	mid-Na–O(2)	1 × 2.34(2)	
	mid-Na–O(2)	1 × 2.64(2)	
	mid-Na–O(1)	1 × 2.75(2)	
	mid-Na–O(2)	1 × 3.10(2)	

ionic radii for Na^{VIII}–O (eight coordination). Moreover, no significant thermal effect is observed for these distances. The Na(1)–O(2) distances are also long: 2.67 Å at 443 K for $x = 2.05$ to be compared with 2.39 Å for Na^{VI}–O (six coordination). But, the Na(1)–O(2) distances highly increase with increasing temperature and, at 623 K for $x = 2.05$, become very close to the Na(2)–oxygen lengths. Concerning the fivefold coordinated mid-Na interstitial site, there is a relatively short average sodium–oxygen distance (2.48 Å) with participation of three oxygens of a face of the NaO_6 octahedron (generally considered as the geometrical bottleneck for the diffusion) and of two oxygens neighboring Na(2) sites.

Figure 6 represents the composition dependence at 443 K of the average sodium–oxygen distances. Upon the substitution of larger Si for P, ⟨Na(2)–O⟩ slightly and continuously increases from 2.648 Å for $x = 0$ to 2.706 Å for $x = 3$. In contrast, as for c hexagonal parameter and Na(1) filling ratio, we note an anomalous behavior for the variation with composition of ⟨Na(1)–O⟩ which presents a maximum near $x = 2$.

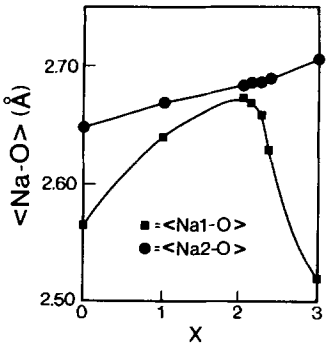

FIG. 6. Composition dependence at 443 K for the average sodium–oxygen distances deduced from the crystal structure determination in the NASICON solid solution $Na_{1+x}Zr_2Si_xP_{3-x}O_{12}$ with $0 \leq x \leq 3$ (crystal data except for $x = 1$; Ref. (*26*)).

(iv) Thermal Vibration Parameters

Anisotropic temperature factor coefficients deduced from the refinements for NASICON $x = 2.05$ single crystals at 443 and 623 K are given in Table V. Sodium atom anisotropies are qualitatively similar to that found in the most previous analysis of the NASICON-type structure. But, at least for Na(1) and Na(2), more reasonable values of temperature factors are obtained. Na(1) exhibits an oblate thermal vibration ellipsoid with a large displacement normal to c which largely increases with temperature. In contrast, Na(2) corresponds to a prolate ellipsoid, weakly dependent on the temperature, with large displacement approximately parallel to c (in fact, slightly inclined to c due to the high U_{23} component). The mid-Na exhibits the expected behavior of an interstitial position within the conduction path with very large thermal components (especially U_{22}, U_{33}, and U_{23}) and a weak temperature dependence. Concerning composition effects, the largest displacement of Na(1) is observed near $x = 2$ and in all the investigated range ($2 < x < 2.4$) the mean-squared displacements of sodium atoms are always very large (0.10 to 0.20 $Å^2$) compared to the ones observed for $x = 3$ at the same temperature (<0.10 $Å^2$).

For the framework ions, it may be noted, in the range $2 < x < 2.4$, that oxygens exhibit relatively high vibration amplitudes (especially for O(1)), almost isotropic and weakly dependent on the temperature, in agreement with a SiO_4/PO_4 tetrahedra disorder. In fact, a dynamic orientational tetrahedra disorder have been displayed in these crystals, above the phase transition, by a Raman study (*13*).

Discussion

We have made a complete X-ray structural investigation of single crystals of intermediate compositions in the NASICON solid solution ($2 < x < 2.4$). The most important result concerns the partial occupation of the interstitial mid-Na position

TABLE V

ANISOTROPIC THERMAL PARAMETERS (Å² × 10⁴)

	U_{11}	U_{22}	U_{33}	U_{12}	U_{13}	U_{23}
			NASICON x = 2.05 at 443 K			
Zr	157(2)	U_{11}	138(2)	$U_{11}/2$	0	0
P–Si	123(4)	136(5)	150(4)	$U_{22}/2$	$U_{23}/2$	38(4)
O(1)	333(16)	456(20)	362(15)	244(15)	−169(14)	4(14)
O(2)	197(11)	244(13)	260(13)	21(10)	77(11)	44(11)
Na(1)	1708(180)	U_{11}	332(100)	$U_{11}/2$	0	0
Na(2)	377(26)	425(39)	2173(143)	$U_{22}/2$	$U_{23}/2$	713(58)
Mid-Na	739(270)	3000(900)	1814(600)	800(590)	530(400)	2200(670)
			NASICON x = 2.05 at 623 K			
Na(1)	3129(410)	U_{11}	183(104)	$U_{11}/2$	0	0
Na(2)	408(21)	524(31)	2281(46)	$U_{22}/2$	$U_{23}/2$	773(61)
Mid-Na	600(200)	2800(500)	1800(400)	150(200)	50(100)	1900(400)

within the conduction path consisting of a network of intersecting channels. The occupation of this position is highly dependent on the composition and can be correlated to the variation of the electrical properties in the NASICON solid solution.

At $x = 0$, only the Na(1) sites are occupied. When increasing the sodium concentration, our results clearly indicate that the x charge compensating sodium ions fill the Na(2) sites. Correlatively a part of Na(1) ions shift toward a vacant Na(2) site. Therefore, it is reasonable to think that the move of sodium ions into the interstitial mid-Na position results from the increase of the interionic repulsions between Na(1) and Na(2) ions. The shift corresponding to a decrease of the Coulombic potential energy.

At about $x = 2$, approximately $\frac{1}{3}$ of the Na(1) sites remains occupied. In fact, for this special composition, we note that each Na(1) site is connected to Na(2) site triangles consisting on average of one vacant site and two filled sites. This association makes possible the shift of all the sites Na(1), as observed at room temperature for the $Na_3Sc_2(PO_4)_3$ monoclinic NASICON analog which is a perfectly stoichiometric $x = 2$ NASICON (*29*). Above $x = 2$, we observed a drastic decrease of the mid-Na occupation which tends to zero for the $x = 3$ end member in which Na(1) and Na(2) positions are fully occupied. It is clear that, in the composition range ($2 < x < 3$), the shift from Na(1) to mid-Na becomes more and more difficult with increasing x, because of the lack of available Na(2) vacant sites. This obviously confirms that the occupation of mid-Na interstitial sites automatically excludes the occupation of neighboring equilibrium Na(2) positions.

All our other significant structural changes with the variation of composition can be deduced from the evolution of the mid-Na interstitial site. The maximum of the average length of the Na(1)–oxygen bond and the maximum of the c hexagonal parameter, observed at about $x = 2$, are clearly associated with the minimum value of Na(1) occupation factor. This is obviously the normal consequence of the presence of a partially occupied site because vacant cationic sites can be equated to negative charges which repulse surrounding oxygen atoms. In the NASICON structure, vacant Na(1) sites lead to increase the height of the Na(1)–O_6 octahedra and to the

associated rotation of SiO_4/PO_4 tetrahedra. Consequently, the successive sodium jumps between sites resulting in the static lattice potential, Na(1) → Na(2) → Na(1), via the shallow potential mid-Na site imply a breathing-like movement of the framework in perfect agreement with the dynamic tetrahedra disorder observed in these crystals (*13*).

In the investigated temperature range, small changes are observed in the sodium distribution with the variation of temperature. We note, with increasing temperature a slight shift of the "mid-Na" position toward the Na(2) position and a slight decrease of the mid-Na occupation factor (0.61 at 623 K for $x = 2.25$ to be compared with 0.67 at 443 K). These results are compatible with the expected decrease of the interionic repulsions when the temperature is raised.

In conclusion, structural determinations in the $Na_{1+x}Zr_2Si_xP_{3-x}O_{12}$ NASICON solid solutions ($0 \leq x \leq 3$) show competing effects of static lattice potential and ion interactions. The Coulomb forces shift a part of Na(1) ions into mid-Na interstitial positions. This displacement is enhanced at $x = 2$ because of both important sodium interactions and high concentration of available interstitial sites. Therefore, the maximum of conductivity at $x = 2$ is directly related to the maximum of the occupation factor of the interstitial mid-Na site. This correlation is in good agreement with stochastic Langevin dynamic simulations of a one-dimensional model for framework ionic conductors proposed by Jacobson *et al.* (*30*), which show that the Coulomb forces push the mobile ions up the crystal framework potential well, lowering the effective potential barrier and increasing the conductivity. This situation is optimized for $x = 2$ in the NASICON solid solution and, consequently, the geometry changes of the framework, which are also a direct consequence of the interionic repulsions, cannot be considered to be the main explanation for the high conductivity at $x = 2$.

References

1. H. Y.-P. Hong, *Mater. Res. Bull.* **11,** 173 (1976).
2. J. B. Goodenough, H. Y.-P. Hong and J. A. Kafalas, *Mater. Res. Bull.* **11,** 203 (1976).
3. J. P. Boilot, J. P. Salanie, G. Desplanches, and D. Le Potier, *Mater. Res. Bull.* **14,** 1469 (1979).
4. J. A. Kafalas and R. J. Cava, "Proceedings of the International Conference on Fast Ion Transport in Solids, Lake Geneva," p. 419, North-Holland, Amsterdam (1979).
5. R. S. Gordon, G. R. Miller, B. J. Mac Entire, E. D. Beck, and J. P. Rasmussen, *Solid State Ionics* **3–4,** 243, (1981).
6. S. Yde-Andersen, J. Lundsgaard, L. Moller, and J. Engell, *Solid State Ionics* **14,** 73 (1984).
7. L. O. Hagman and P. Kierkegaard, *Acta Chem. Scand.* **22,** 1822 (1986).
8. R. G. Sizova, A. A. Voronkov, N. G. Shumyatskaya, V. V. Ilywkhin, and N. Belov, *Sov. Phys. Dokl.* **17,** 618 (1973).
9. D. Tran Qui, J. J. Caponni, and J. C. Joubert, *J. Solid State Chem.* **31,** 219 (1981).
10. J. P. Boilot, G. Collin, and R. Comes, *J. Solid State Chem.* **50,** 91 (1983).
11. H. Kohler, H. Schultz, and O. Melnikov, *Mater. Res. Bull.* **18,** 1143 (1983).
12. P. R. Rudolf, A. Clearfield, and J. D. Jorgensen, *Solid State Ionics* **21,** 213 (1986).
13. Ph. Colomban, *Solid State Ionics* **21,** 97 (1986).
14. J. P. Boilot, G. Collin, and Ph. Colomban, *Mater. Res. Bull.* **22,** 669 (1987).
15. V. Von Alpen, M F. Bell, and W. Wickelhaus, *Mater. Res. Bull.* **14,** 1317 (1979).
16. B. J. Wuensh, L. J. Schioler, and E. Prince, "Proceedings of the Conference on High Temperature Solid Oxide Electrolytes, August 16–17, 1983," Vol II, "Cations Conductors" (F. J. Salzano, Ed.), p. 55, Brookhaven (1983).
17. H. Kohler and H. Schulz, *Mater. Res. Bull.* **20,** 1461 (1985).
18. G. Lucazeau, M. Barj, J. L. Soubeyroux, A. J. Dianoux, and C. Delmas, *Solid State Ionics* **18, 19,** 959 (1986).
19. F. Cherkaoui, G. Villeneuve, C. Delmas, and P. Hagenmuller, *J. Solid State Chem.* **65,** 293 (1986).
20. M. Barj, H. Perthuis, and Ph. Colomban, *Solid State Ionics* **11,** 157 (1983).
21. H. Perthuis and Ph. Colomban, *Ceram. Int.* **12,** 39 (1986).

22. J. A. IBERS AND W. C. HAMILTON, Eds., "International Tables for X-ray Crystallography," p. 148, International Union of Crystallography, Kynoch Press, Birmingham (1974).
23. G. COLLIN *et al.*, to be published.
24. C. K. JOHNSON, *in* "International Tables for X-ray Crystallography," p. 313, International Union of Crystallography, Kynoch Press, Birmingham (1974).
25. W. C. HAMILTON, *in* "International Tables for X-ray Crystallography," p. 287, International Union of Crystallography, Kynoch Press, Birmingham (1974).
26. W. H. BAUR, J. R. DYGAS, D. H. WHITMORE, AND J. FABER, *Solid State Ionics* **18, 19,** 935 (1986).
27. J. ALAMO AND R. ROY, *Amer. Ceram. Soc.* **5,** 78 (1984).
28. J. J. DIDISHEIM, E. PRINCE, AND B. J. WUENSCH, *Solid State Ionics* **18, 19,** 944 (1986).
29. G. COLLIN, R. COMES, J. P. BOILOT, AND PH. COLOMBAN, *J. Phys. Chem. Solids* **47,** 843 (1986).
30. JACOBSON, H. SOLOMON, MARK A. RATNER, AND A. NITZAN, *Phys. Rev. B* **23,** 1580 (1981).